JOURNAL OF MECHANICAL ENGINEERING AND SCIENCES (JMES)
ISSN: 2289-4659 e-ISSN: 2231-8380
VOL. 14, ISSUE 2, 6822 – 6834
DOI: https://doi.org/10.15282/jmes.14.2.2020.22.0534

ORIGINAL ARTICLE

Effect of corrosion on mechanical properties of the joining of materials

M. K. G. Abbas[1], Galal M. Abdella[1], Elsadig. O. Eltai[1] and M Gul[2]

[1] Department of Mechanical and Industrial Engineering, Qatar University, Doha, Qatar
Phone: +97444037388; Fax: +97444034301
[2] Department of Mechanical Engineering, Faculty of Engineering & Technology, Bahauddin Zakariya University, Multan-60000, Pakistan.

ABSTRACT – The effect of corrosion behavior in critical environmental conditions on the mechanical properties of composite/metal materials joints was investigated by immersing metalic materials into 5wt% hydrochloric acid solutions. The current study was carried out on a single lab joint with a total thickness of 4mm; thus, a destructive test was undertaken to investigate the corrosion behavior induced degradation of mechanical properties followed by Scanning electron microscope analysis (SEM). The joined specimens were examined under both non-corrosive and corrosive environmental conditions. Moreover, the Taguchi analysis of experimental data for maximizing the required output is carried out to validate the impact and significance of input factors. Experimental results have shown that the weight losses of the mild steel and aluminum materials are 7.45% and 16.7%, respectively, in 5% wt hydrochloric acid after three weeks. The corrosive environment affected the strength of the joints and obtained an early failure on the joint region that leads to a reduction on the strength of the materials by almost 15% compared to the non-corroded joint. The joining of non-corroded similar steel obtained the highest maximum stress among all other specimens, where the maximum recorded stress was 140.5MPa as compared to 125MPa for corroded specimen. Furthermore, the mode of failure and hardness tests were obtained and analyzed for all specimens. A significant reduction in the hardness of the materials after exposure to the HCl acid was observed.

ARTICLE HISTORY
Revised: 24th Oct 2019
Accepted: 20th Nov 2019

KEYWORDS
Corrosion;
joining;
dissimilar materials;
failure analysis;
mechanical properties.

INTRODUCTION

Over the years, modern automobile manufacturers have sought to achieve the highest levels of performance and efficiency by designing safe and stable vehicle bodies using environmentally friendly materials. They also seek to reduce fuel consumption and thus reduce carbon dioxide emissions by designing a lightweight vehicle [1]. These demands encouraged researchers in the automotive industry to look for techniques to design robust, lightweight and reliable structures [2–5]. One of the possible techniques that can be used to design a lightweight vehicle is by joining dissimilar materials. The use of lightweight materials with distinct physical and chemical properties has opened up a new field of research for the joining of different materials. However, joining techniques such as ultrasonic joining [6], fusion welding [7], and joining by plastic deformation [8] are unable to joint metal to fiber reinforced polymer materials.

In the joining of metal to non-metal materials, various joining approaches have been introduced. A flow drill screw (FDS) is a mechanical bonding method that can be used with or without the pre-drilled hole. FDS was used early by Audi automotive company to join aluminum components on the TT production with the required of pre-drilled holes, and on the R8 without pre-drilled holes [9]. Friction stir blind riveting (FSBR) is an alternative technique for joining dissimilar material which does not involve a pre-drilled hole. By a high-speed, a blind rivet rotates on the surface of the workpiece causing the rivet to be pushed across the stack-up under decreased force [10]. FDS and FSBR were developed to join similar and dissimilar materials. However, the FSD technique needed the material to be heated by a rotating screw to enable penetration, which may cause a change in the mechanical properties of the metal. Due to the high penetration forces used in the FSBR technique, it requires support on the backside of the overlap area of the workpiece [11, 12]. These types of joining techniques have limitations on their applications when it is challenging to use them in the joining of closed structures. Subsequently, the mechanical fastening technique is a suitable method to reduce production time and cost [12].

One of the most widely used techniques for joining similar and dissimilar materials is the mechanical fastening joining technique. This technology has a significant advantage over other technologies that the ease of disassembly for maintenance, repair or remanufacturing, where it does not lead to the demolition of the components [13]. Bolted joints are designed for either shear load, tensile, or a mixture of both. When the force applied is parallel to the bolt, the joints are called tensile joints. The shear joint is therefore when the force applied is perpendicular to the axis of the bolt [9]. The mechanical fastening techniques that use bolt or rivet for joining purposes have various methods on the joining of dissimilar materials such as scarf [14], tapered [15], single, and double lap joints [15–17].

*CORRESPONDING AUTHOR | M. K. G. Abbas | ✉ mohdgaab@gmail.com

In a single lap joint, two symmetrically bonded materials are bonded together by utilizing bolt, rivet or both [18]. Many studies have been conducted to test the lab joining either numerically or experimentally, using various techniques. Streitferdt et al. [19] studied the shear strength of the co-cured and adhesive bonded steel joined to CFRP undergone to tensile load. This investigation results showed that adhesive bonding increases the tensile shear strength of single-lap joints. Grant et al. [20] used the numerical and experimental methods to study the effect of three and four points bending tests of the single lap joints. The results showed no failure in the four points bending test, while the adhesive yielded in the three-point bending observation. In another study, Abbas and co-workers [21] compared the adhesive joining technique with combined adhesive and mechanical joining techniques to examine the strength of the double lap joint of dissimilar materials. They found that the holes created in the specimens for inserting mechanical fasteners caused a lower strength compared to the adhesive joining technique. They found that the holes formed in the specimens to insert mechanical fastener caused a decrease in strength compared to the technique of adhesive joining.

Even though the joining of CFRP and metal make the mechanical properties of the structure highly attractive, several factors may affect the joining of dissimilar materials and cause limitations on the industrial applications. Corrosive environment, humidity, and high temperature are external factors that influence the joining strength [22, 23]. Corrosion of steel is the main environmental hazard for steel structures. Corrosion can result in a reduction in the mechanical properties of the steel, especially in its ductility. In the same context, steel corrosion can lead to minimizing the steel structure lifetime, which causes structural failure [24–28].

The relationship among the mechanical properties and corrosion characterization of the bonded materials is not always obvious, which makes the long-term performances of the joined structure are difficult to predict. Therefore, it is an important aspect that estimating the impact of corrosion behavior on mechanical performance to allow engineering designers to understand the choice of suitable materials for the production of homogeneous or heterogeneous joints [29–32]. There is lacking research to identify the declination mechanism of the mechanical properties of the joining of metal to CFRP materials due to metal corrosion. The changes in the metal microstructural characterization due to corrosion degradation are the main factor affecting the mechanical properties of the metal [24].

To the best of our knowledge, the impact that corrosion may have on the joining materials has not been well studied, in fact, this article is meant to be part of series of articles that aims at studying the impact of corrosion using different corrosion environments with different concentrations at different temperatures. The purpose of the current study is to evaluate the effect of the corrosive environment on the mechanical properties and failure mechanisms of the bolt joint for the joining of similar and dissimilar materials.

The strategy of mechanical joining was carefully chosen in this study in order to joint the composite with the metal, the reasons for choosing it because it is widely used in industry, it has also low cost and easy accessibility comparing to other strategies such as ultrasonic joining, fusion welding, and joining by plastic deformation, Moreover, mechanical joining is easy to disassemble which made it attractive for repair, recycle and inspection purposes. After finishing the series of the planned papers, authors are planning to make an Atlas for the impact of corrosion on different joining materials that exposed to a different environment that will serve the industry in Qatar and elsewhere.

EXPERIMENTAL SETUP AND ANALYSIS

Materials and Fabrication

The investigation has been accomplished on single lap joint specimens made from mild steel, aluminum, and carbon fiber-reinforced polymer with a total joint thickness of 4mm. A bolt made of steel with a 6mm diameter was used in the design to connect two parts to form the single lap joint specimen as shown in Figure 1(a). Mild steel material that is used for a wide range of different applications was used as a test metal material along with aluminum. Specimens were manufactured from the supplied sheets manually and by machining. Each specimen was cut into 80mm x 30mm x 2mm. The work plan involved two groups of specimens to be tested. One group of specimens joined and tested without exposing to any corrosive environment, while specimens in the other group were immersed in the hydraulic acid solution, then joined to examine the effect of corrosive environment on the joining strength. The investigation was composed of the manufacturing of a single lap joint with mild steel, aluminum, and CFRP materials. The specimens were divided into two groups, with and without exposing to a corrosive environment. The effect of the single lap joint was estimated after specimens were subjected to static loading. Failure mechanisms of the single lap joint were observed and discussed. A comparison of the strength of the specimens with and without exposing to the corrosive environment was established.

Experimental Setup

Joint's strength was tested by doing tensile tests for all samples on a universal testing machine, INSTRON 5585H. The tensile tests were conducted at room temperature under displacement-controlled crosshead with a speed of 1mm/min. As shown in Figure 1(b), with a crosshead distance of 55mm, the flat rectangular samples were held vertically. The total length of the specimen is 160mm with a width of 30mm, whereas the length of the gage was 50mm. The load capacity of the machine can reach the load cell of 100kN; therefore, the general aim of the tensile test was to pull to brake setup. The microstructures of the fractured joint surfaces were analyzed using a scanning electron microscope.

Hardness test was carried out on Rockwell hardness equipment with a load of 60kg, a ball indenter of 1/16 inch diameter, and a duration of 10s using indentec hardness tester Model 8187.LKV. UK. Different readings were taken around the joining area after the specimens were exposed to a tensile load; the same number of readings was then taken at an interval of 1mm away from the joining area.

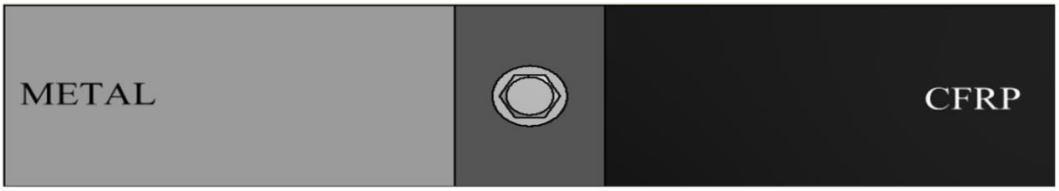

(a) The final design of bolted joint of metal and CFRP.

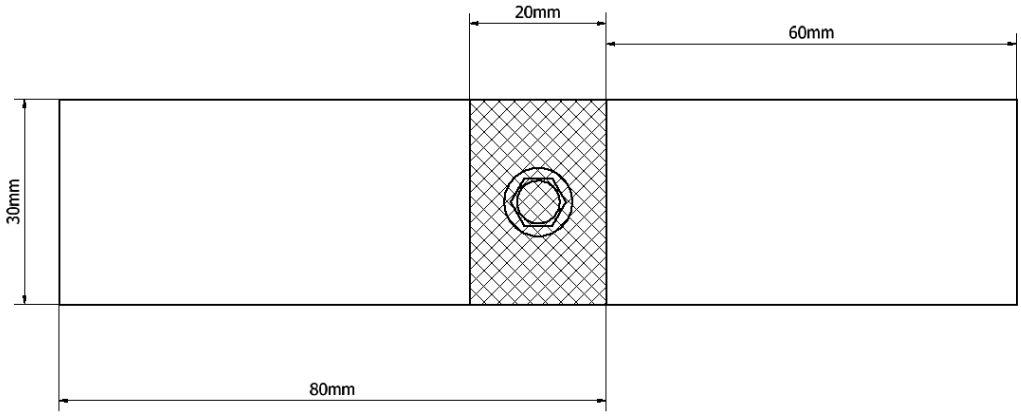

(b) Single lap joint geometry where the overlap length is 20 mm, the bolt hole diameter is 6 mm.

Figure 1. Typical joining method.

Immersion Test

The concentration of Hydrochloric acid that used for corrosion simulation at room temperature was 5% wt to quantify the mechanical properties degradation of the single lap joint. Specimens'surfaces were cleaned with alcohol and then dried before immersing in the acid solution. The immersion duration was set for three weeks for all specimens. The specimens were weighed before immersing in the acid solution to determine the original weight to compare it after corrosion occurred. After the specimens are withdrawn from the acid solution, they were cleaned using distilled water and dried by air, by using a microbalance of 0.01g resolution, the weight change was measured. The loss in weight of the specimens was calculated to determine the corrosion rate.

Taguchi Analysis

Taguchi's analysis of experimental data for maximizing the required output was carried out in Minitab-18 by choosing "larger the better" criteria to validate the impact and significance of input factors in terms of S/N ratios [33–36]. Signal to Noise (S/N) Ratio with 'larger is better' criteria has the following standard Eq. (1).

$$S/N = -10 \times \log 10\ (\text{sum}(1/Y^2)/n) \quad (1)$$

Here 'n' is the total no of observations of the given data as presented in Table 4. While 'Y' represents the output response against each input variable.

EXPERIMENTAL RESULTS AND DISCUSSION

Corrosion Rate

For calculating the corrosion rate of the metal materials, Eq. (2) is used:

$$\text{Corrosion rate} = \frac{534W}{\rho At} \quad (2)$$

where, the corrosion rate is expressed in (mpy), W is the weight loss in (g), ρ is the density of the carbon steel (7.85g/cm^3), A is the total surface area in (inch^2), and t is the period of immersion in (hours).

The weight losses of the specimens were determined as an indication of the corrosion rate. Eq. (2) is used to calculate the corrosion rate of the mild steel and aluminum in 5% wt hydrochloric acid solution at room temperature. The weight losses of the mild steel and aluminum materials are 7.45% and 16.7%, respectively, in 5% wt hydrochloric acid after three weeks. The immersion test found that the corrosion rate of the mild steel is closer to that in aluminum, where the corrosion rate calculated of the mild steel found to be 0.05mpy. Whereas 0.046mpy is a corrosion rate calculated for aluminum material. Based on the percentages of the weight loss of both metal materials, it can be predicted that the corrosion rate will increase with the increase of hydrochloric acid concentration; consequently, the materials' weight will decrease with the increase of the immersion period.

It is worth to mention that, the current study sheds some light on the impact of the corrosion on the mechanical properties of materials that were joined by bolt joining. It is also worth mentioning that this type of joing may have a negative impact on the corrosion process, in other words, it may increase the corrosion rate because the chance for the occurrence of crevice corrosion is big as the corrosive acid is expected to penetrate under the bolts and being trapped there. This will create different aeration cells, in other words, the amount of oxygen within the crevice is going to be different from the acid outside the crevice. The un-pleasant about crevice corrosion is that it developed underneath the both without being visually observed or detected until sever failure occurred. This should be taken into account when using this type of joing.

Mechanical Properties Evaluation for Bolted Joining

For all samples, a static loading was conducted to establish a baseline for comparing the stress rate. After the tensile test was completed, the ultimate tensile stress was recorded. The information on each specimen's tensile characteristics was summarized in Table 1 below. All specimens were loaded in tension and tested up to failure with a velocity rate of 1mm/min. Figure 2 shows the stress-strain curves of all specimens joined by the mechanical fastening technique.

Tensile test results, for similar and dissimilar joining materials, concluded that the material of mild steel has high strength than the pure aluminum (Al) material. This can be seen in the corroded, and non-corroded combinations of similar steel/steel and dissimilar steel/CFRP have the highest stress than those in the combinations of similar Al/Al and dissimilar Al/CFRP. However, the joining of non-corroded similar steel/steel obtained the highest maximum stress among all other specimens, where the maximum stress recorded was 140.5MPa. The stress-strain behavior elucidates that the non-corroded specimens detect a higher failure strength compared to corroded specimens. Furthermore, non-corroded steel/steel has a maximum load than corroded steel/steel with a percentage of 11.03. The lower failure strength was found to be in the joint of dissimilar Al/CFRP and similar Al/Al, which can be attributed to the weakness of the aluminum material compared to other materials. The weakness of the aluminum material was determined when yielded at the lowest load applied.

Generally, the mechanical bolt joints had either a ductile or a brittle fracture. The joining samples containing steel had a brittle fracture, while the joining of aluminum had a ductile fracture owing to the nature of both metal components. However, the highest stress for steel/CFRP is almost twice the total stress of Al/CFRP. Furthermore, in all cases, the stress-strain curve of the steel specimen shows a sharp peak, while the aluminum specimen shows a slight rounding at the top due to the ductility of the aluminum and the stiffness of the steel material. Although the tensile test velocity was 1mm/min, the failure of the steel joints took more time than aluminum failure. In the end, it was noticed that the corrosive environment influenced the strength of the metal materials; it reduced the strength of the materials to almost 15% of the original strength. However, the bolts involved in the joining of materials that required pre-drilled to create bolt hole were the cause of the failure due to the stress was concentrated on the hole leading to a crack that eventually caused the failure.

Table 1. Mechanical Properties of bolted joint obtained from the tensile experiment.

	Combinations	Elastic modulus (GPa)	Maximum Load (kN)	Ultimate tensile stress (MPa)	Extension (mm)
Non-Corroded	Similar Steel/Steel	4.09	8.43	140.5	4.19
	Similar Al/Al	1.28	2.18	36.4	9.43
	Dissimilar Steel/CFRP	2.77	5.46	91.1	9.89
	Dissimilar Al/CFRP	1.41	2.94	49.0	10.83
	Similar CFRP/CFRP	1.26	3.57	59.5	10.75
Corroded	Similar Steel/Steel	2.86	7.5	125.0	4.71
	Similar Al/Al	1.24	1.88	31.3	7.75
	Dissimilar Steel/CFRP	2.33	4.7	78.3	9.68
	Dissimilar Al/CFRP	0.99	1.81	30.2	7.25

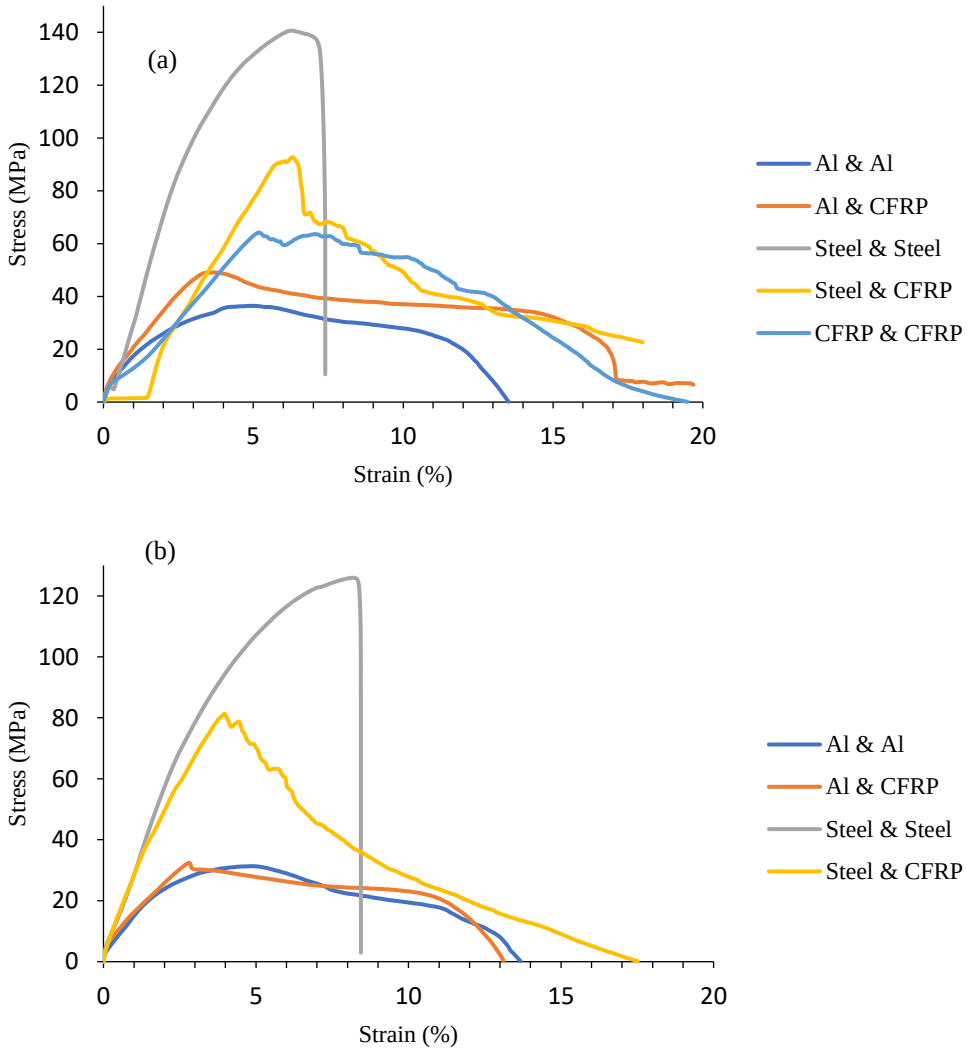

Figure 2. The stress-strain curve: (a) non-corroded specimens, (b) corroded specimens.

Failure Mode

The failure mode is a very significant parameter to prevent a failure mechanism when the concept implemented in actual life. The failure mode is a significant element of mechanical reaction that is often used in design factors. Figure 3 demonstrates the most prevalent failure modes in the mechanical fastening and how the geometric structure impacted them [30].

The failures mode was obtained from a tensile experiment into different types of the adherend, Failures were observed for specimens were exposed to the corrosive environment when the specimens immersed in the hydraulic acid solution are shown in Figure 4. The failure mode of the specimens that were not exposed to any corrosive environment are shown in Figure 5. It is important to understand that when a single lap joining technique is used, the applying load is transferred from one adherend to another in the bolted joint. From the failure observations, the bolted joint stayed firmly inserted in the specimens during the tensile test in the similar and dissimilar joints of the aluminum and CFRP. The carried load in the similar combinations of corroded and non-corroded aluminum joining experienced a shear out failure mode, this failure caused the yield to the aluminum plate around the bolted joint. After reaching the maximum tensile load, the bolted joint experienced load reduction and considerable damage in the aluminum plate on the dissimilar joining of aluminum and CFRP in both corroded and non-corroded aluminum. This failure observed a shear failure mechanism. However, a non-corroded aluminum plate showed a shear out and then yielding in the adherend as shown in Figure 5(a). On the contrary, for the joining of mild steel and CFRP, the failures were observed on the CFRP plates even in the case when the mild steel pre-exposed to the hydraulic acid solution, which was not predictable. These types of failure mechanisms identified as shear out failure. On the opposite side, thesimilar mild steel elucidates the highest joint failure strength when bearing failures were noticed in the case of corroded and non-corroded mild steel. The primary failure occurred on the bolt joint that caused the bearing failure on the mild steel plates, Figure 4 (d) and Figure 5(d) illustrated the bolt failure due to the tensile experiment.

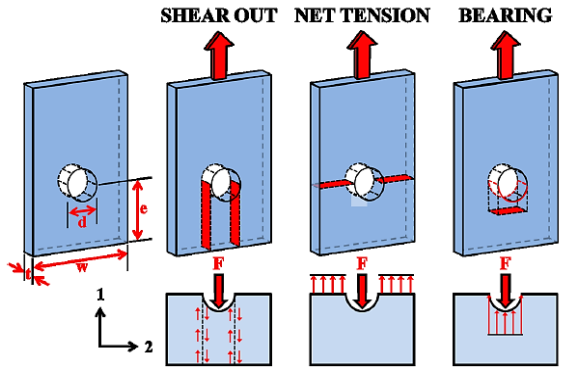

Figure 3. Failure modes for mechanical fastener joint [37].

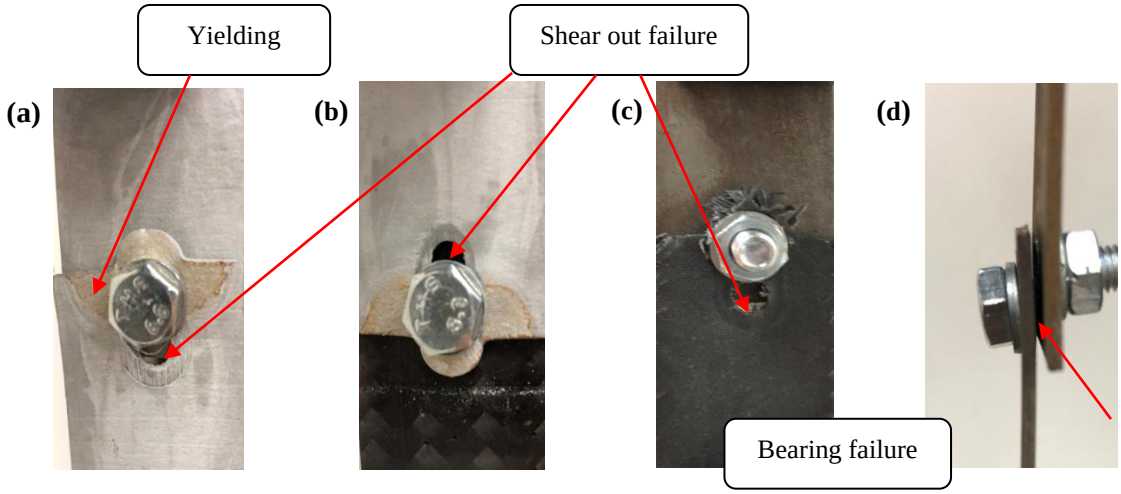

Figure 4. Failure mechanism of bolted joint for corroded specimens, (a) Al/Al, (b) Al/CFRP, (c) steel/CFRP, (d) steel/steel.

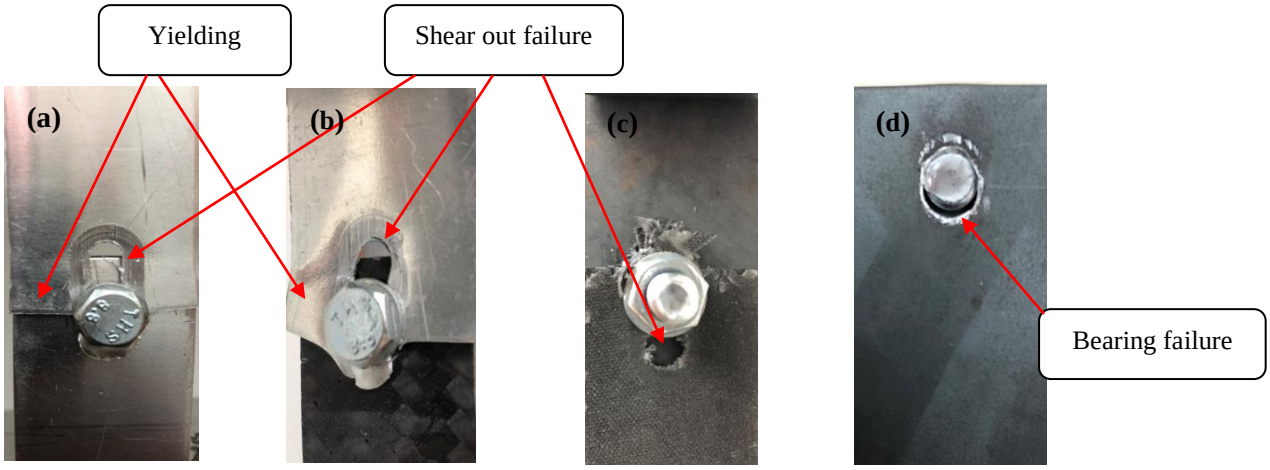

Figure 5. Failure mechanism of bolted joint for non-corroded specimens, (a) Al/Al, (b) Al/CFRP, (c) steel/CFRP, (d) steel/steel.

Hardness Analysis

Hardness is an essential property that widely used to evaluate the mechanical properties for different metals. Currently, the hardness test was achieved to estimate the effect of corrosion and tensile test on the bolted joints of similar and dissimilar materials. The specimen was tested in five different places around the bolted area which were illustrated

in Figure 6. The variations in the hardness values of all specimens are shown in Table 2, while the hardness profiles comparison for each combination of the corroded and non-corroded specimen is shown in Figures 7.

Non-Corroded combination joints expressed a good hardness value. For similar steel specimens, a reduction was observed in the hardness value in the corroded specimen by around 50% compared to the non-corroded specimen. The highest hardness value recorded on non-corroded was 70HFR. However, the value obtained in the area of point 3 has the lowest hardness value in both cases, which means that the area has the maximum stress compared to other areas. Surprisingly, there is a convergence on the hardness value obtained from the combinations of similar corroded and non-corroded aluminum. However, there is a significant difference in the value of the hardness determined in area 5 about 13HFR; this difference is occurred due to the yielded area that took place because of the tensile experiment. On the other hand, the measured hardness value on the dissimilar steel/CFRP specimens shows an increase in hardness on the specimen that was not exposed to any corrosive environment. The lowest hardness value of 30HFR was found to be in area 3 of the corroded specimen, which is the area that has the highest stress. Whereas, a comparison of hardness values of corroded and non-corroded dissimilar aluminum/CFRP specimens showed that the corroded aluminum has the lowest values on all the measured areas. The lowest hardness values 23HFR and 26HFR of the corroded and non-corroded aluminum specimens respectively were found to be in area 5, where the aluminum plate yielded due to the tensile load applied.

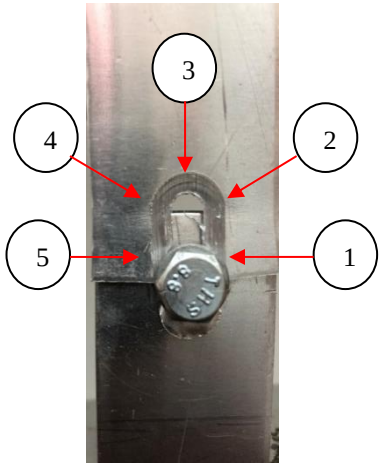

Figure 6. The position of the hardness test value.

Table 2. Hardness value for non-corroded and corroded specimens.

	Combinations	Measured Area (HFR)				
		1	2	3	4	5
Non-Corroded	Similar Steel/Steel	70	48	24	59	62
	Similar Al/Al	38	53	45	49	50
	Dissimilar Steel/CFRP	49	47	52	58	58
	Dissimilar Al/CFRP	40	60	44	45	26
Corroded	Similar Steel/Steel	60	25	19	27	31
	Similar Al/Al	35	50	40	47	37
	Dissimilar Steel/CFRP	38	35	30	47	37
	Dissimilar Al/CFRP	32	46	38	44	23

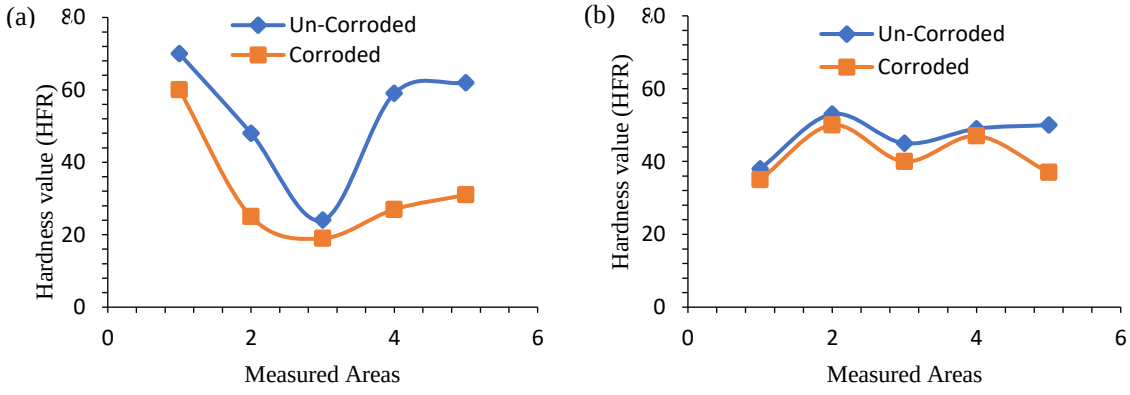

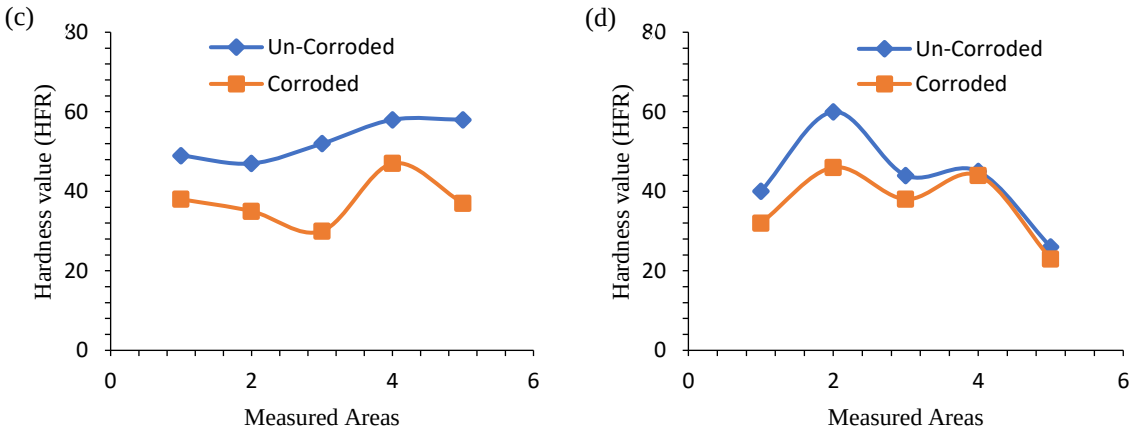

Figure 7. Hardness profile for corroded and non-corroded specimens: (a) steel/steel, (b) Al/Al, (c) steel/CFRP, (d) Al/CFRP.

Failure surface analysis defines the type and location of failure due to the applied tensile load. The surface morphology of the joint of similar and dissimilar joining was observed by SEM. SEM images of the tensile fracture surface of a failed bolted joint are shown in Figure 8 and Figure 9. The location of the failure for the corroded and non-corroded steel specimens was taken of similar mild steel joining, and it was found to be on the bolted area that caused bearing failure. The cavity can be found in the direction of the load applied to the fracture surface owing to the reduce energy absorption before fracture and less plastic deformation.

The microstructure fracture surface of the CFRP is taken after the tensile experiment of the joining of dissimilar corroded and non-corroded mild steel/CFRP at 2500x, as revealed in Figure 8 (a), (b). The fracture happened in the region of the bolt, where the crack began from the bolt hole. The SEM pictures indicated that the fiber pulled out fiber by a tensile test. It can be observed that the pullout took place in various areas and the same orientation. SEM images demonstrate some consistency in the microstructure of the CFRP.

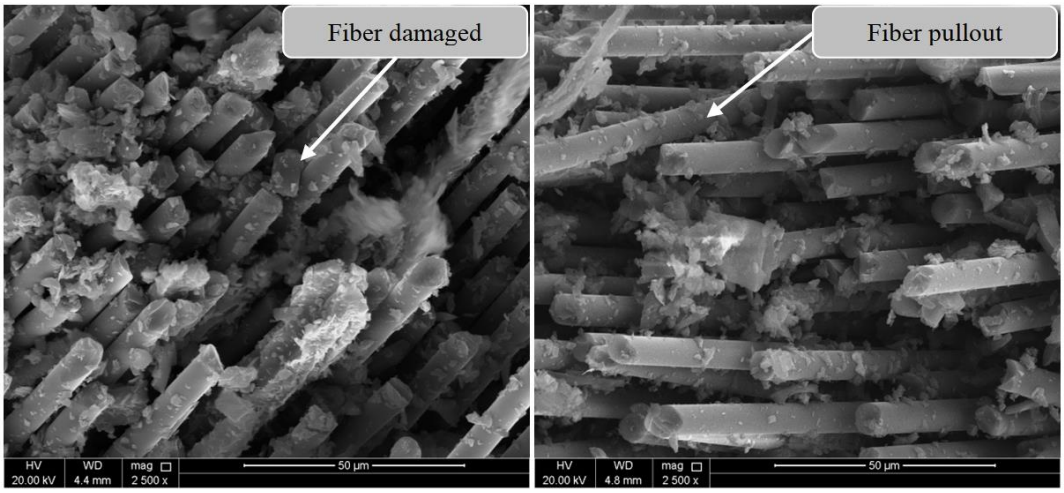

(c) non-corroded steel/CFRP (d) corroded steel/CFRP

Figure 8. SEM micrographs of steel specimens.

Using visual observation, the crack started from the bolt region. This will highlight the broken fibers shown in the SEM images as shown in Figure 9 (a). The fracture surface of the carbon fiber was disturbed, which was clarified as the fibers were not uniformly elongated. Because of its weakness compared to non-corroded aluminum, It appears that the corroded aluminum influenced the carbon fabrics and can be proved in the SEM image in Figure 9(b) that taken at 2500x, which indicates that the fabric was elongated. The SEM images for corroded and non-corroded aluminum fracture surfaces which were taken at 2500x are shown in Figure 9 (c), (d), respectively. The ductile fracture is a widespread plastic deformation before cracking when the fracture in the ductile material remains constant until the applied load increases. However, the non-corroded aluminumsurfacehasa homogenous interface. While the SEM image of corroded

aluminum that shown in Figure 9 (c)elucidated inhomogeneous fracture surface. Additionally, some cracks on the surface may occur owing to the bolt impact that a pre-drilled hole is needed.

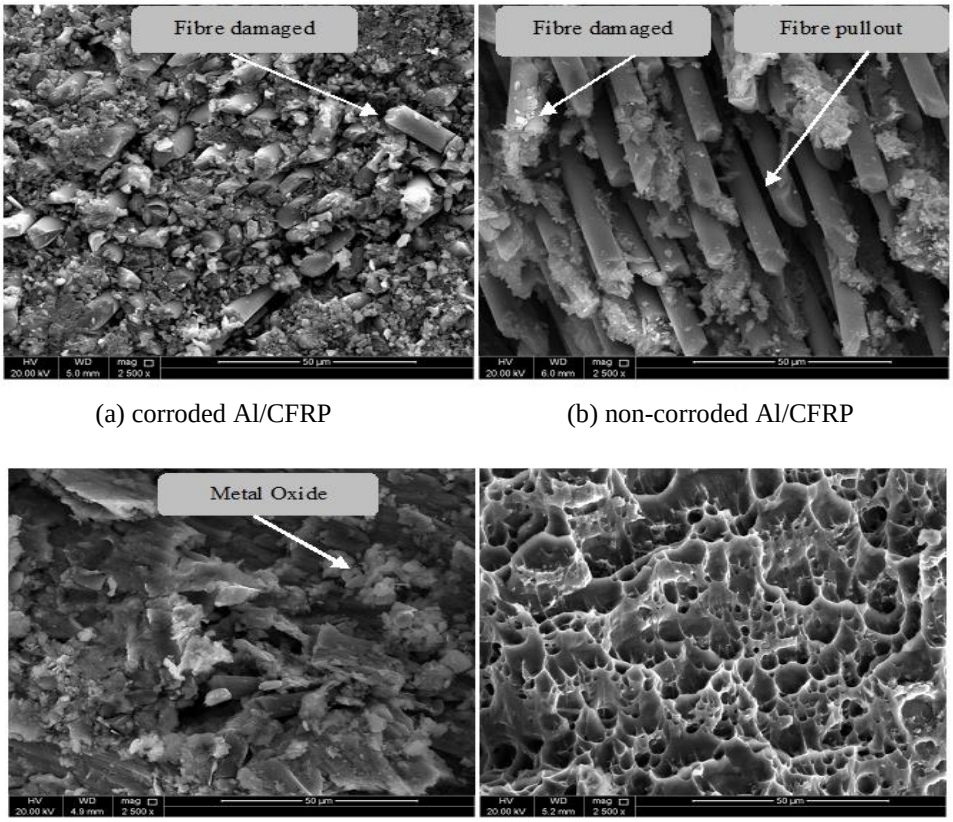

(a) corroded Al/CFRP (b) non-corroded Al/CFRP

(c) corroded Al/Al (d) non-corroded Al/Al

Figure 9. SEM micrographs of aluminum specimens.

Taguchi Analysis

Taguchi analysis is a well-known method for studying variation. Using the Taguchi method for optimizing the setting parameters of the experimental work is common in literature [33]. In this paper, three input parameters with their corresponding levels of variations are considered, as mentioned in Table 3.

Table 3. Input parameters with levels of variation.

Input Parameters	Code	Levels (L)			
		L-1	L-2	L-3	L-4
Type of Environment	A	Corroded	Non-corroded	-	-
Type of Materials	B	Steel/Steel (SS)	Al/Al (AA)	Steel/CFRP (SC)	Al/CFRP (AC)
Loading Rate (N)	C	500	1000	1500	2000

This paper uses the L32 (2^1*4^2) mixed-level as presented in Table 4, and tensile strength, as output response, is calculated experimentally and recorded in Table 4.

Table 4. The orthogonal Array L_{32} Design with output response.

Sr #	Type of Environment	Type of Material	Loading Rate (N)	TensileStrength (MPa)
1	Corroded	SS	500	8.31
2	Corroded	SS	1000	16.71
3	Corroded	SS	1500	24.99

4	Corroded	SS	2000	33.60
5	Corroded	AA	500	8.34
6	Corroded	AA	1000	16.80
7	Corroded	AA	1500	24.98
8	Corroded	AA	2000	31.55
9	Corroded	SC	500	8.53
10	Corroded	SC	1000	16.65
11	Corroded	SC	1500	24.98
12	Corroded	SC	2000	33.30
13	Corroded	AC	500	8.41
14	Corroded	AC	1000	16.68
15	Corroded	AC	1500	24.96
16	Corroded	AC	2000	33.44
17	Non-corroded	SS	500	8.35
18	Non-corroded	SS	1000	16.65
19	Non-corroded	SS	1500	25.00
20	Non-corroded	SS	2000	33.45
21	Non-corroded	AA	500	8.37
22	Non-corroded	AA	1000	16.70
23	Non-corroded	AA	1500	24.98
24	Non-corroded	AA	2000	33.35
25	Non-corroded	SC	500	8.45
26	Non-corroded	SC	1000	16.71
27	Non-corroded	SC	1500	24.98
28	Non-corroded	SC	2000	33.42
29	Non-corroded	AC	500	8.57
30	Non-corroded	AC	1000	16.70
31	Non-corroded	AC	1500	24.99
32	Non-corroded	AC	2000	33.42

All these experimental results of Table 4 are analyzed in MINITAB software to validate the impact and significance of input factors in the form of S/N ratios. The target of the analysis was to find the optimal set of input parameters, which increases tensile strength.

The larger-is the better response table for the signal to noise ratios (S/N ratio's)is shown in Table 5. Table 5(a) and (b) give the rank wise impact of the input factors, which shows that the loading rate is a more sensitive and important factor for determining the tensile strength of joining materials, while the corroded and non-corroded environment is the least significant factor with rank 3.

Table 5. Response tables for (a) Signal to noise ratios (b) Mean "larger is better".

(a)

Level	Type of Environment	Type of Materials	Loading Rate
1	25.31	25.33	18.50
2	25.35	25.27	24.45
3	--	25.36	27.95
4	--	25.36	30.42
Delta	0.04	0.09	11.92
Rank	3	2	1

(b)

Level	Type of Environment	Type of Materials	Loading Rate
1	20.764	20.883	8.416
2	20.881	20.634	16.700
3	--	20.877	24.982
4	--	20.896	33.191
Delta	0.116	0.263	24.775
Rank	3	2	1

In Taguchi design, control factors (process input parameters) are identified from their robustness so that variability can be reduced by minimizing the effect of noise factors (uncontrolled factors). This design suggests an optimal combination of control factors that resists the variation caused by noise factors. This optimal setting is determined from the higher S/N (signal-to-noise) ratio of each control factor to reduce variability. Here the goal of experiments was to get high tensile strength, so ''Larger is better" criteria were selected to calculate S/N ratio.

Optimization by Taguchi is a two-step process. In the first step,S/N ratios of each input factor were measured to recognize those control factors that play a vital role in reducing variability. The second step involves the identification of those control factors that calculate the mean to minimize the variability effect on the signal-to-noise ratio, as shown by Figure 10.

The most favorable (optimal) combination of input factors is assessed by considering the larger values of SN ratio and mean plots, as given in figure 10. Response graphs of the SN ratio's help in defining the significant level of the best

performance. According to these graphs, non-corroded 'SC' and 'AC' type of materials with a maximum loading rate of 2000 N have more tensile strength. Moreover, it showed that non-corroded dissimilar combination of materials gives maximum tensile strength than corroded similar materials; the same result is also validated experimentally.

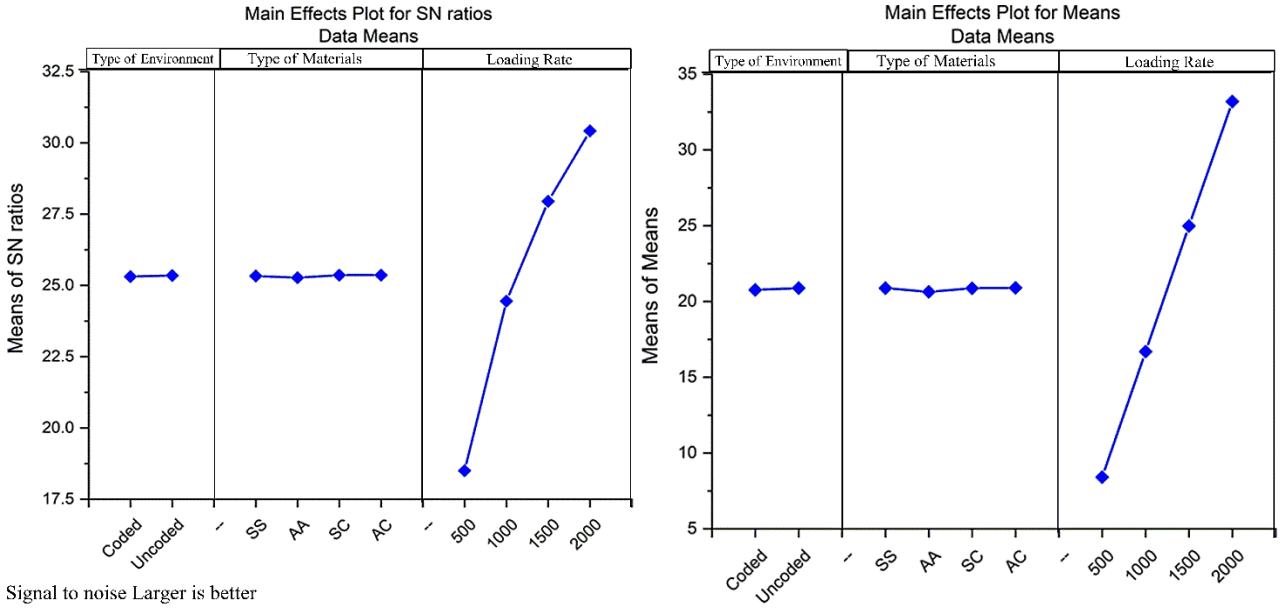

Figure 10. SN ratio plot for an optimal combination of input factors.

CONCLUSION

Based on the experimental research conducted in the present work, the following conclusions can be drawn.

- A comparison of corrosive and non-corrosive samples revealed a significant difference in the mechanical properties of bolted joints.
- Joining of similar mild steel material gave the highest failure strength in both cases of corroded and non-corroded compared to the aluminum material, which found to be the weakest combination observed in this study.
- The combination of non-corroded aluminum showed more strength as compared to the combination of corroded aluminum.
- Non-corroded specimens expressed a good hardness value. However, a reduction was observed in some measured areas on the hardness value in the corroded specimen by around 50% compared to the non-corroded specimen.
- The failure mechanism of joining areas showed that all failures were observed around bolt areas, which means that the holes which were created for the bolts, promoted the failure mechanism.
- Bearing and shear-out failure were identified in the steel and aluminum adherend, respectively.
- The corrosive environment affected the mechanical properties of the metal materials immersed in HCl solution when they were tested by a tensile experiment. Corrosion degradation showed a significant reduction in the mechanical properties and changes in the microstructures.
- It was also confirmed and validated from the Taguchi analysis that all non-corroded materials give high tensile strength, while corroded materials showed low strength.
- Taguchi technique is an efficient way to validate the impact and significance of input factors by using MINITAB.

ACKNOWLEDGMENT

This paper was funded by internal grant No. QUSD-CENG-2018\2019-5 from Qatar University fund. The statements made herein are solely the responsibility of the authors.

REFERENCES

[1] K. Mori and Y. Abe, "A review on mechanical joining of aluminium and high strength steel sheets by plastic deformation," *Int. J. Light. Mater. Manuf.*, vol. 1, no. 1, pp. 1–11, 2018, doi: 10.1016/j.ijlmm.2018.02.002.

[2] N. Osman, Z. Sajuri, and M. Z. Omar, "Multi-pass friction stirred clad welding of dissimilar joined AA6061 aluminium alloy and brass," *J. Mech. Eng. Sci.*, vol. 12, no. 4, pp. 4285–4299, 2018, doi: 10.15282/jmes.12.4.2018.22.0368.

[3] J. Zhang, K. Chaisombat, S. He, and C. H. Wang, "Hybrid composite laminates reinforced with glass/carbon woven fabrics for lightweight load bearing structures," *Mater. Des.*, vol. 36, pp. 75–80, 2012, doi: 10.1016/j.matdes.2011.11.006.

[4] M. K. G. Abbas, A. Niakan, C. C. Ming, R. Singh, and P. Teo, "Design and numerical analysis of leaf spring using composite materials," *Key Eng. Mater.*, vol. 723, no. 305, p. 310, 2017, doi: 10.4028/www.scientific.net/KEM.723.305.

[5] N. Sakundarini, Z. Taha, S. H. Abdul-Rashid, and R. A. R. GhaziFtablela, "Optimal multi-material selection for lightweight design of automotive body assembly incorporating recyclability," *Mater. Des.*, vol. 50, pp. 846–857, 2013, doi: 10.1016/j.matdes.2013.03.085.

[6] J. M. Munoz-Guijosa, G. Nanaumi, K. Ohtani, and N. Ohtake, "Perpendicular ultrasonic joining of steel to aluminium alloy plates," *J. Mater. Process. Technol.*, vol. 243, pp. 112–122, 2017, doi: 10.1016/j.jmatprotec.2016.12.010.

[7] F. Adnan, Z. Sajuri, and M. Z. Omar, "Effect of uniaxial load on microstructure and mechanical properties of Thixo-joint AISI D2 tool steel," *J. Mech. Eng. Sci.*, vol. 13, no. 2, pp. 5006–5020, 2019, doi: 10.15282/jmes.13.2.2019.17.0414.

[8] J. P. M. Pragana, C. M. A. Silva, I. M. F. Bragança, L. M. Alves, and P. A. F. Martins, "A new joining by forming process to produce lap joints in metal sheets," *CIRP Ann.*, vol. 67, no. 1, pp. 301–304, 2018, doi: 10.1016/j.cirp.2018.04.121.

[9] K. Martinsen, S. J. Hu, and B. E. Carlson, "Joining of dissimilar materials," *CIRP Ann. - Manuf. Technol.*, vol. 64, pp. 679–699, 2015, doi: 10.1016/j.cirp.2015.05.006.

[10] H. A. Khan, W. M. Wang, K. Wang, S. Li, S. Miller, and J. Li, "Investigation of mechanical behavior of dissimilar material FSBR joints exposed to a marine environment," *J. Manuf. Process.*, vol. 37, pp. 376–385, 2019, doi: 10.1016/j.jmapro.2018.12.011.

[11] J. Min, J. Li, Y. Li, B. E. Carlson, J. Lin, and W. M. Wang, "Friction stir blind riveting for aluminum alloy sheets," *J. Mater. Process. Technol.*, vol. 215, pp. 20–29, 2015, doi: 10.1016/j.jmatprotec.2014.08.005.

[12] J. Min, Y. Li, B. E. Carlson, S. J. Hu, J. Li, and J. Lin, "A new single-sided blind riveting method for joining dissimilar materials," *CIRP Ann. - Manuf. Technol.*, vol. 64, pp. 13–16, 2015, doi: 10.1016/j.cirp.2015.04.047.

[13] S. A. Tekalur, A. VanderKlok, W. Zhang, and A. Dutta, "Evaluating bolted joint strength at high strain rates," in *Conference Proceedings of the Society for Experimental Mechanics Series*, 2012, pp. 1–4, doi: 10.1007/978-1-4614-4553-1_1.

[14] H. Adin, "The investigation of the effect of angle on the failure load and strength of scarf lap joints," *Int. J. Mech. Sci.*, vol. 61, pp. 24–31, 2012, doi: 10.1016/j.ijmecsci.2012.04.010.

[15] F. A. Stuparu, D. A. Apostol, D. M. Constantinescu, C. R. Picu, M. Sandu, and S. Sorohan, "Local evaluation of adhesive failure in similar and dissimilar single-lap joints," *Eng. Fract. Mech.*, vol. 183, pp. 39–52, Oct. 2017, doi: 10.1016/j.engfracmech.2017.05.029.

[16] J. Li, Y. Yan, T. Zhang, and Z. Liang, "Experimental study of adhesively bonded CFRP joints subjected to tensile loads," *Int. J. Adhes. Adhes.*, vol. 57, pp. 95–104, 2015, doi: 10.1016/j.ijadhadh.2014.11.001.

[17] M. Mariam, M. Afendi, M. S. Abdul Majid, M. J. M. Ridzuan, and A. G. Gibson, "Tensile and fatigue properties of single lap joints of aluminium alloy/glass fibre reinforced composites fabricated with different joining methods," *Compos. Struct.*, vol. 200, pp. 647–658, 2018, doi: 10.1016/j.compstruct.2018.06.003.

[18] X. Shang, E. A. S. Marques, J. J. M. Machado, R. J. C. Carbas, D. Jiang, and L. F. M. da Silva, "Review on techniques to improve the strength of adhesive joints with composite adherends," *Compos. Part B Eng.*, vol. 177, p. 107363, 2019, doi: 10.1016/j.compositesb.2019.107363.

[19] A. Streitferdt, N. Rudolph, and I. Taha, "Co-Curing of CFRP-Steel Hybrid Joints Using the Vacuum Assisted Resin Infusion Process," *Appl. Compos. Mater.*, vol. 24, pp. 1137–1149, 2017, doi: 10.1007/s10443-016-9575-3.

[20] L. D. R. Grant, R. D. Adams, and L. F. M. da Silva, "Experimental and numerical analysis of single-lap joints for the automotive industry," *Int. J. Adhes. Adhes.*, vol. 29, pp. 405–413, 2009, doi: 10.1016/j.ijadhadh.2008.09.001.

[21] M. K. G. Abbas, N. Sakundarini, and I. Kong, "Optimal Selection for Dissimilar Materials using Adhesive Bonding and Mechanical Joining," *IOP Conf. Ser. Mater. Sci. Eng.*, vol. 469, p. 012051, 2019, doi: 10.1088/1757-899X/469/1/012051.

[22] D. Borrie, H. B. Liu, X. L. Zhao, R. K. Singh Raman, and Y. Bai, "Bond durability of fatigued CFRP-steel double-lap joints pre-exposed to marine environment," *Compos. Struct.*, vol. 131, pp. 799–809, 2015, doi: 10.1016/j.compstruct.2015.06.021.

[23] E. Mahdi and E. Eltai, "Development of cost-effective composite repair system for oil/gas pipelines," *Compos. Struct.*, vol. 202, pp. 802–806, 2018, doi: 10.1016/j.compstruct.2018.04.025.

[24] L. Li, M. Mahmoodian, C. Q. Li, and D. Robert, "Effect of corrosion and hydrogen embrittlement on microstructure and mechanical properties of mild steel," *Constr. Build. Mater.*, vol. 170, pp. 78–90, 2018, doi: 10.1016/j.conbuildmat.2018.03.023.

[25] E. O. Eltai, F. Musharavati, and E. S. Mahdi, "Severity of corrosion under insulation (CUI) to structures and strategies to detect it," *Corros. Rev.*, vol. 37, no. 6, pp. 1–12, 2019, doi: 10.1515/corrrev-2018-0102.

[26] E. Mahdi, A. Rauf, and E. O. Eltai, "Effect of temperature and erosion on pitting corrosion of X100 steel in aqueous silica slurries containing bicarbonate and chloride content," *Corros. Sci.*, vol. 83, pp. 48–58, 2014, doi: 10.1016/j.corsci.2014.01.021.

[27] E. Mahdi, E. O. Eltai, and A. Rauf, "The impact of metal inert gas welding on the corrosion and mechanical behavior of AA 6061 T6," *Int. J. Electrochem. Sci.*, vol. 9, pp. 1087–1101, 2014.

[28] E. Eltai, K. Al-Khalifa, A. Al-Ryashi, E. Mahdi, and A. S. Hamouda, "Investigating the corrosion under insulation (CUI) on steel pipe exposed to Arabian Gulf sea water drops," *Key Eng. Mater.*, vol. 689, pp. 148–153, 2016, doi: 10.4028/www.scientific.net/KEM.689.148.

[29] L. Calabrese, E. Proverbio, G. Galtieri, and C. Borsellino, "Effect of corrosion degradation on failure mechanisms of aluminium/steel clinched joints," *Mater. Des.*, vol. 87, pp. 473–481, 2015, doi: 10.1016/j.matdes.2015.08.053.

[30] V. Bystrianský, A. Krausová, J. Macák, J. Děd, E. Eltai, and A. M. Hamouda, "Beneficial effect of shot peening on steamside oxidation of 300-series austenitic steels: An electrochemical study," *Appl. Surf. Sci.*, vol. 427, pp. 680–685, 2018, doi: 10.1016/j.apsusc.2017.08.035.

[31] E. S. Mahdi and E. O. Eltai, "Study on the impact of welding on the corrosion properties of AA 6061 T6," *Appl. Mech. Mater.*, vol. 575, pp. 210–213, 2014, doi: 10.4028/www.scientific.net/AMM.575.210.

[32] E. Eltai, E. Mahdi, and A. Alfantazi, "The effects of gas tungsten arch welding on the corrosion and mechanical properties of AA 6061 T6," *Int. J. Electrochem. Sci.*, vol. 8, pp. 7004–7015, 2013.

[33] R. A. Kishore, R. Tiwari, A. Dvivedi, and I. Singh, "Taguchi analysis of the residual tensile strength after drilling in glass fiber reinforced epoxy composites," *Mater. Des.*, vol. 30, pp. 2186–2190, 2009, doi: 10.1016/j.matdes.2008.08.035.

[34] N. I. S. Hussein, S. Laily, M. S. Salleh, and M. N. Ayof, "Statistical analysis of second repair welding on dissimilar material using Taguchi method," *J. Mech. Eng. Sci.*, vol. 13, pp. 5021–5030, 2019, doi: 10.15282/jmes.13.2.2019.18.0415.

[35] G. M. Abdella, K. Yang, and A. Alaeddini, "Multivariate adaptive approach for monitoring simple linear profiles," *Int. J. Data Anal. Tech. Strateg.*, vol. 6, pp. 2–14, 2014, doi: 10.1504/IJDATS.2014.059012.

[36] M. Jamil and E. Y. K. Ng, "Ranking of parameters in bioheat transfer using Taguchi analysis," *Int. J. Therm. Sci.*, vol. 63, pp. 15–21, 2013, doi: 10.1016/j.ijthermalsci.2012.07.002.

[37] C. C. Chamis, "Simplified procedures for designing composite bolted joints," *Soc. Plast. Ind. Reinf. Plast. Institute, Annu. Conf. - Proc.*, vol. 9, no. 6, pp. 614–626, 1990, doi: 10.1177/073168449000900607.